Sensor Design for Inductive Proximity and Moving Direction Sensing of Metal Targets

Cristinel Ababei and James E. Richie

Department of Electrical and Computer Engineering
Marquette University, Milwaukee WI, USA
Email: {cristinel.ababei,james.richie}@marquette.edu

***Abstract*—We present the design of a new inductive proximity sensor to detect metal targets and their direction of movement. The proposed sensor design includes a base board with the necessary microcontroller based circuitry for driving and reading the sensing LC tanks and several different solutions for the printed sensor coil. Different coil configurations are fabricated on separate printed circuit boards designed to plug-and-play into the base board. They are intended for different specific applications including for sensing metal targets approaching perpendicularly on the coil plane and for sensing and identifying the lateral direction of movement (i.e., left-to-right or right-to-left). The coil designs are studied via simulations using the freely available Numerical Electromagnetics Code (NEC). A complete hardware prototype is developed and demonstrated to detect different metal targets, including copper, brass, aluminum, and stainless steel. It is also shown that measurements obtained from hardware experiments are in good agreement with the simulations.**

***Index Terms*—inductive sensor, proximity sensing, printed coil, Atmega32p, inductance to digital converter**

I. Introduction

Inductive sensors exploit the principle of electromagnetic coupling between the coil and the metal target. Some electromagnetic energy is transferred into the target when the target enters the electromagnetic field produced by the sensor coil [1]. This energy causes the occurrence in the metal target of circulating eddy currents that induce reverse electromagnetic field on the sensor coil, which is usually connected in parallel with a capacitor to form an LC tank circuit. During operation, the capacitor is charged by a short pulse, after which the LC sensor starts to oscillate. As a consequence of the reverse electromagnetic field, the effective inductance of the sensor coil is reduced. The reduction in the coil inductance results into a shift in the resonant frequency of the tank, which in turn leads to a change in the amplitude of the signal across the coil. This change can be detected and interpreted as the fact that the metal target approached and entered the sensor's proximity. Inductive proximity sensors (IPS) offer several advantages over capacitive and optical technologies including: reliable operation in harsh environmental conditions, resistance to contamination, immunity against oil, water and dirt, low cost due to the magnet-free sensing, high temperature range, and maintenance-free operation [2], [3].

II. Related Work

Most of the traditional proximity sensing approaches used a discrete coil component with a magnetic core to form the primary LC tank, which suffers from large volumes and higher costs. In an effort to address those limitations, printed circuit board (PCB) coils have been introduced. While most of the proximity sensor solutions focused on detecting metallic targets, some studies proposed proximity sensors with the capability of detecting both metal and non-metal targets [4], [5]. Previous studies investigated also how temperature affects the overall performance of the sensor, including the thermal drift for different sensing distances [4]. Temperature sensors were used also to develop techniques for self-calibration and compensation for temperature effects [3]. For special applications, previous studies investigated printing the sensor coil on flexible substrates to allow the sensor to be attached on non-planar surfaces [6], [7].

III. Proposed Sensor Design and Hardware Prototyping

A simplified block diagram of the base board of the proposed sensor design is shown in Fig. 1.a. In this paper, we study two different LC tank configurations, shown in Fig. 1.b and Fig. 1.c. The LC tank from Fig. 1.b is used to detect targets that approach the coil plane perpendicularly. The sensor from Fig. 1.c is intended for use in applications where information about the moving direction in addition to proximity detection is needed. An individual LC tank is formed by a printed circuit board coil inductor and a surface mounted device capacitor connected in parallel with the inductor.

The based board includes the microcontroller unit (MCU), which runs all the firmware algorithms. To reduce the number of components, we use an inductance-to-digital converter based approach. This is similar to previous studies in [2], [11]. The MCU base board includes primarily the Atmega328p microcontroller [12] and the LDC1101 inductance-to-digital converter (LDC) [13] from Texas Instruments (TI). For further cost reduction (i.e., use only one instance of the LDC converter), a one-to-two analog switch is included to enable the connection of the LDC converter to the LC tanks on the sensor boards shown in Fig. 1.b and c. Thus, one or two LC tanks can be connected to the inductance to digital converter via the programmable 1-to-2 bidirectional switch (TI TS5A23157). In addition, the base board includes a programmable clock generator (Maxim DS1077L), which is programmed via I2C from the MCU to supply a 10 MHz clock signal to the LDC

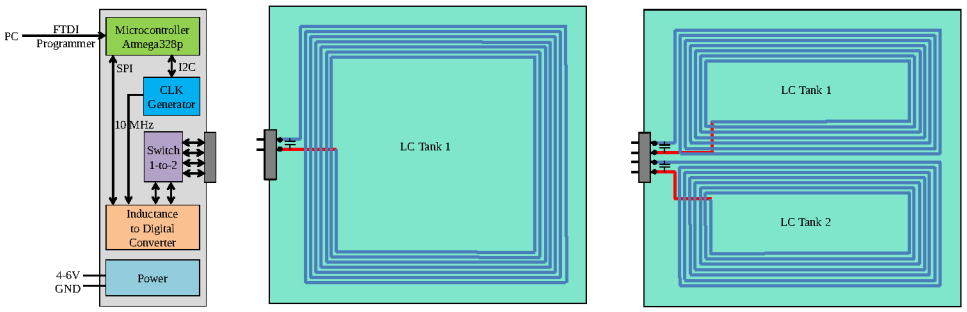

(a) (b) (c)

Fig. 1. a) The main microcontroller base board of the proposed sensor design, b) Single printed circuit board coil, c) Dual printed circuit board coil topologies.

converter. The MCU configures and talks to the inductance to digital converter via SPI. The first generation prototype of the proposed design is shown in Fig. 2.

IV. Firmware Development

The firmware executed by the microcontroller is developed with the capability of detecting which of the sensor boards shown in Fig. 1.b and c is connected to the base board. This capability makes the design to be a plug-and-play solution where the base board will know to adjust on the fly the appropriate main algorithm. The flowchart that describes the algorithms executed for each of the two cases is shown in Fig. 3. The inductance to digital converter can be configured to operate in two different modes. In LHR operation mode, the LDC converter measures inductance (L) with high resolution. In RP+L operation mode the converter can measure parallel resistance (RP) and inductance (L) [13].

When the sensor board from Fig. 1.b is attached to the base board, the sensor will detect metal targets approaching the sensor perpendicularly to the sensor plane. The algorithm executed in this case is described in the left-hand side of the flowchart from Fig. 3. Its main idea is to iteratively poll the inductance to digital converter and to calculate the resonance frequency of the LC tank, *fSENSOR*. When a metal target approaches the sensor, the frequency *fSENSOR* increases - due to the change in inductance as a result of the eddy current induced into the metal target and therefore of the electromagnetic coupling thus created. It is this change in frequency, which if larger than a certain threshold is used to indicate to the user that the metal target approached the sensor.

In the other case, when the sensor board from Fig. 1.c is attached to the base board, the sensor will be used to detect metal targets moving from left-to-right or from right-to-left in front of the sensor plane but within detectable distance. The algorithm executed in this case is described in the right-hand side of the flowchart from Fig. 3. It is similar to the algorithm used in the first case, which here is essentially used alternatively for each of the two LC tanks, each with its own resonant frequency.

V. Simulations

There are well-known formulas to estimate the inductance of a printed loop or spiral geometry (see, for example, [8]). However, as a proximity sensor, another important characteristic is the extent of the magnetic field above the coil. A strong field is needed to sufficiently induce eddy currents and hence a measurable change in inductance.

Let the coil in Fig.1.b be in the $x - y$ plane. Since eddy currents will circulate around the time-changing $\vec{H}$, the direction of interest for the magnetic field $\vec{H}$ is the z direction. The strength of $\vec{H}$ due to a wire loop of current is conveniently characterized using the magnetic dipole moment, which is proportional to the current and the area of the loop. A larger area admits a larger H_z. Multiple turns having the same area would be ideal. However, in a PCB scenario, a multi-layer board may be too expensive. Therefore, here, a single layer board is considered. To keep the area of each turn as large as possible, a spiral geometry is proposed.

A spiral inductance can be modeled as a set of coplanar loops of current, each with the same current. Since the total spiral length is very small compared to wavelength, the phase of the current is roughly constant. The freely-available Numerical Electromagnetics Code, NEC [9] was used to model thin wires in square loops and observe the simulated H_z above the loop. Fig. 4 shows H_z as a function of height above the center of the loop. Three different square loops were considered, each with the same current. The current was chosen so that $H_z = 1$ at the center of the smallest loop. As shown in Fig. 4, H_z is largest in the center of each loop; however, H_z falls very fast for the smallest loop, and as the loop size increases, H_z falls more slowly. Note that the total field falls close to linearly as the height increases from 0 to 2 cm. This characteristic may be useful to calibrate the proximity sensor and estimate the distance between the sensor and a metal object. The calibration will require knowledge of the metal, since the conductivity (and hence the eddy currents) will depend on the density of free electrons.

VI. Experiments

A. Hardware Experiments

We conducted experiments using the prototype shown in Fig. 2. In our testing, we used four different types of metal targets: aluminum 6061, copper 110, brass C360, and stainless steel 304 - each with dimensions of 1/4" x 2" x 6" (Thickness x Width x Length).

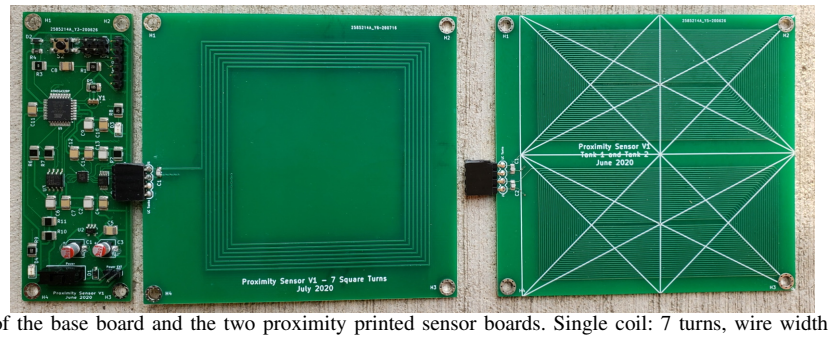

Fig. 2. Hardware prototypes of the base board and the two proximity printed sensor boards. Single coil: 7 turns, wire width 0.508 mm, wire spacing 0.762 mm. Dual coils: 14 turns, wire width 0.254 mm, wire spacing 0.381 mm. Complete design files can be found at [14].

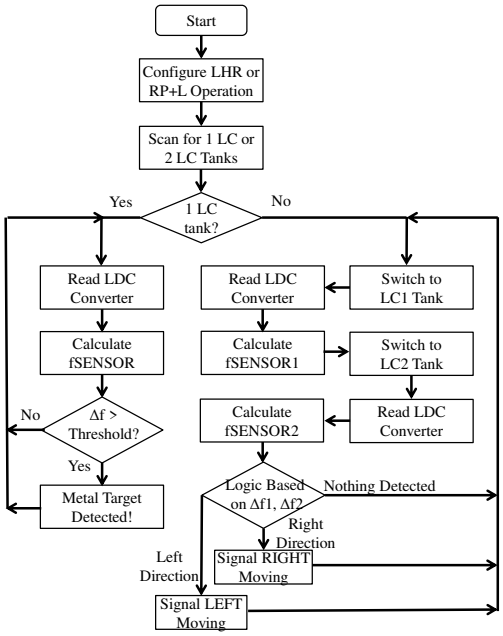

Fig. 3. Flowchart of the intelligent firmware executed on the microcontroller - it automatically detects if the sensor board attached to the base board has one LC tank only or two LC tanks.

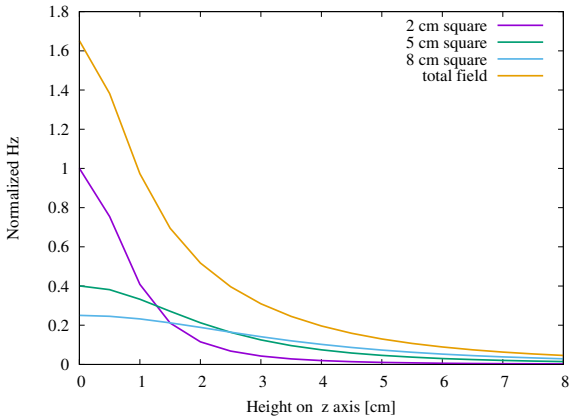

Fig. 4. Simulated magnetic field H_z for three different square loop sizes: 2 cm, 5 cm, 8 cm, and their sum (3.25 in is approximately 8.26 cm).

In the first experiment, we use the single LC tank sensor board from Fig. 2, which is used to detect metal targets approaching perpendicularly the sensor plane. The experimental

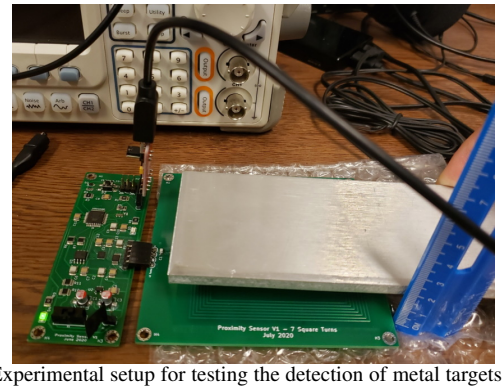

Fig. 5. Experimental setup for testing the detection of metal targets approaching the proximity sensor.

setup is shown in Fig. 5. A plastic ruler is used to measure the distance between the metal target and the sensor plane, measured perpendicularly to the plane of the printed PCB coil. The metal target is moved towards the sensor plane symmetrically along a perpendicular line in the center of the sensor plane. The first time during this movement when the base board senses the metal target, the red LED on the base board turns on to indicate the detection. The distance between the metal target and the sensor plane measured by the ruler at that time is recorded and reported in Table I. In addition to the red LED lighting-up to indicate the detection of the metal target, short text messages are printed in a serial terminal on the host PC (i.e., a laptop) via the FTDI converter that is also used for the programming of the base board.

TABLE I
MAXIMUM DISTANCES WHERE METAL TARGETS ARE DETECTED AS THEY APPROACH PERPENDICULARLY TO THE SENSOR PLANE.

Metal Target	Max. Dist. [mm]
Aluminum	25
Copper	30
Brass	30
Stainless Steel	35

In order to plot the variation of the resonant frequency, *fSENSOR*, of the single LC tank sensor with the distance between the metal target and the sensor plane, we record the resonant frequency values as the metal target moves towards the sensor plane. The results obtained for the single LC tank sensor board with each of the four different types of

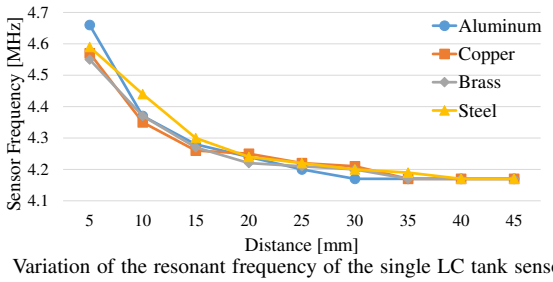

Fig. 6. Variation of the resonant frequency of the single LC tank sensor with the distance between the metal target and the sensor plane.

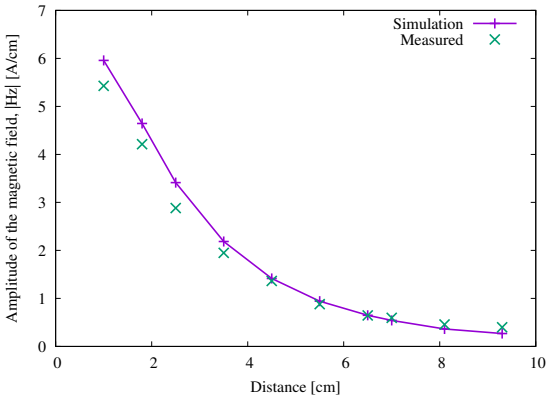

Fig. 7. Magnetic field in the z direction: experiments vs. simulations.

metal targets are shown in Fig. 6. During this experiment an oscilloscope is used to measure the sensor frequency across the LC tank.

In the second experiment, we use the dual LC tank sensor board from Fig. 2, which is used to detect lateral movement of the metal targets. The proximity sensor successfully detects left-to-right and right-to-left movement of the targets. However, due to lack of space, we do not include here detailed results. Complete documentation, hardware and firmware source files, as well as a video demonstration are made publicly available at [14].

B. Hardware Measurements Versus Simulations

In this section, we report on the comparison between the measurements of the magnetic field near the single LC tank sensor board prototype from Fig. 2 and the values estimated via simulations. These values are measured along the z direction, on a line perpendicular in the center of the sensor plane. Figure 7 shows the amplitude of the magnetic field H_z [A/cm] as the distance above the center of the coil grows from 1 to 9 cm. The agreement between simulation and measurement is quite good. As mentioned previously, we see that H_z falls linearly over the first 3 cm above the coil in both simulation and the measured data.

VII. Discussion and Future Work

We observed that the proposed proximity sensor design (prototyped as shown in Fig. 2) successfully detects different metal targets approaching the sensor on a perpendicular direction to the sensor plane. We also observed that hardware measurements are in good agreement with the simulations of the near-field magnetic field, measured along the z direction, perpendicular to the sensor plane.

As future work, we plan to integrate the capability of detecting both metal and non-metal targets into the proposed sensor design [4], [5], Also, we plan to develop light-versions of machine learning (ML) techniques and integrate them into the main firmware algorithm to be able to distinguish between different types of metals. Finally, while the simulations used in this paper are to quantify and validate the operation of the sensor coils, a custom in-house simulation framework can be used to conduct a simplified design space exploration (DSE) in order to find out the best combination of parameter values that result in the best performance of the tank circuit. Currently, we plan to investigate design parameters such as the width of the printed conductor wire (W), the spacing between adjacent conductors (S), and the total number of turns (N).

VIII. Conclusion

A new inductive proximity sensor design that uses printed circuit board coils to detect the presence of metal targets and their moving direction was presented. A hardware prototype was created and used successfully in experiments to detect the approaching and the lateral movement of metal targets of aluminum, copper, brass, and stainless steel. Hardware measurements were found to be in agreement with the simulations of the near-field magnetic field generated by the sensor board.

References

[1] Inductive Sensing Guide, Cypress, AN219207, 2019. [Online]. Available: https://www.cypress.com/documentation/application-notes/an219207-inductive-sensing-design-guide.

[2] Inductive Proximity Switch BoosterPack, TIDUAY3A, Texas Instruments, 2015. [Online]. Available: http://www.ti.com/lit/ug/tiduay3a/tiduay3a.pdf.

[3] M. Jagiella and S. Fericean, "Miniaturized inductive sensors for industrial applications," *IEEE Int. Conference on Sensors*, 2002.

[4] D.G. Silva, J.A. Justino Ribeiro, and T.C. Pimenta, "Design of eddy current sensor IC for large displacement," *IEEE Int. Symposium on Industrial Electronics*, 2013.

[5] J. Long and B. Wang, "A metamaterial-inspired combined inductive-capacitive sensor," *Applied Physics Letters*, vol. 106, no. 074104, 2015.

[6] X. Chen and T. Ding, "Flexible eddy current sensor array for proximity sensing," *Sensors and Actuators A: Physical*, vol. 135, no. 1, pp. 126-130, March 2007.

[7] N. Jerance, N. Bednar, and G. Stojanovic, "An Ink-Jet Printed Eddy Current Position Sensor," *MDPI Sensors*, vol. 13, no. 4, pp. 5205-5219, 2013.

[8] Thomas K. Ishii, Ed., "Handbook of Microwave Technology, Volume 1", Academic Press, New York NY, 1995.

[9] Gerry J. Burke, "Numerical Electromagnetics Code (NEC) – Method of Moments – Parts I, II, and III", UCID-18834, Lawrence Livermore National Laboratories, Jan. 1981.

[10] MEEP - a free finite-difference time-domain (FDTD) simulation software package, MIT, 2017. [Online]. Available: http://ab-initio.mit.edu/wiki/index.php/Meep.

[11] S. Zuk, A. Pietrikova, and I. Vehec, "Development of planar inductive sensor for proximity sensing based on LTCC," *IEEE Int. Spring Seminar on Electronics Technology (ISSE)*, 2016.

[12] ATmega328P8-bit AVR Microcontroller with 32K Bytes In-System Programmable Flash, Atmel Microchip, 2019. [Online]. Available: https://www.microchip.com/wwwproducts/en/ATmega328p

[13] LDC1101, 1.8V, High Resolution Inductance to Digital Converter, Texas Instruments, 2019. [Online]. Available: http://www.ti.com/product/LDC1101.

[14] Proximity Sensor Design for Detection of Metal Targets and Direction of Moving, 2020. [Online]. Available: http://dejazzer.com/hardware.html.